following programs: Zalkin's FORDAP Fourier program, Busing and Levy's ORFFE function and error program, and Ibers NUCLS least-squares program. Plots of the structures were drawn with the aid of C. K. Johnson's ORTEP. Neutral atom scattering factors were taken from D. T. Cromer and J. B. Mann, *Acta Crystallogr., Sect. A*, **24**, 321 (1968). Hydrogen atom scattering factors were taken, "International Tables for X-Ray Crystallography", Vol. III, Kynoch Press, Birmingham, England, 1962. Anomalous scattering corrections were applied to heavy atoms and were taken from D. T. Cromer, *Acta Crystallogr.*, **18**, 17 (1965).
(29) G. Germain and M. M. Woolfson, *Acta Crystallogr., Sect. B*, **24**, 91 (1968).
(30) B. F. Hoskins, S. A. Mason, and J. C. B. White, *Chem. Commun.*, 554 (1969); M. J. Hamor, T. A. Hamor, and J. L. Hoard, *J. Am. Chem. Soc.*, **86**, 1938 (1964); L. E. Webb and E. B. Fleischer, *J. Chem. Phys.*, **43**, 3100 (1965).
(31) S. Silvers and A. Tulinsky, *J. Am. Chem. Soc.*, **86**, 927 (1964).
(32) V. L. Goedken, S. M. Peng, J. Molin-Norris, and Y.-A. Park, *J. Am. Chem. Soc.*, in press.
(33) J. L. Hoard, *Science*, **174**, 1295 (1971).
(34) L. J. Radonovich, A. Bloom, and J. L. Hoard, *J. Am. Chem. Soc.*, **94**, 2073 (1972).
(35) J. L. Hoard, G. H. Cohen, and M. D. Glick, *J. Am. Chem. Soc.*, **89**, 1992 (1967).
(36) B. Gonzalez, J. Kouba, S. Yee, C. Reed, J. Kirner, and W. R. Scheidt, *J. Am. Chem. Soc.*, **97**, 3247 (1975).
(37) M. D. Glick, G. H. Cohen, and J. L. Hoard, *J. Am. Chem. Soc.*, **89**, 1996 (1967).
(38) J. L. Hoard, M. J. Hamor, T. A. Hamor, and W. S. Caughey, *J. Am. Chem. Soc.*, **87**, 2312 (1965).
(39) V. L. Goedken, J. Molin-Case, and Y.-A. Whang, *J. Chem. Soc., Chem. Commun.*, 337 (1973).
(40) V. L. Goedken, Y.-A. Park, and M. Weiss, submitted for publication.
(41) F. Hanic, M. Handlovic, and O. Lindgren, *Collect. Czech. Chem. Commun.*, **37**, 2119 (1972).

Effects of Peripheral Steric Constraints and Metal Ion Size on the Structure of Three Five-Coordinate Macrocyclic Ligand Complexes of the Type $[M(C_{22}H_{22}N_4)X]$, M = Co(III), Fe(III), Mn(II); X = I, Cl, $N(C_2H_5)_3$

Marvin C. Weiss, Bruce Bursten, Shie-Ming Peng, and Virgil L. Goedken*[1]

Contribution from the Department of Chemistry, University of Chicago, Chicago, Illinois 60637. *Received May 19, 1976*

Abstract: The crystal and molecular structures of three five-coordinate complexes of the dianionic macrocyclic ligand $C_{22}H_{22}N_4^{2-}$ have been determined from three-dimensional x-ray diffraction data. The complexes, together with their pertinent crystal data are: $[Co(C_{22}H_{22}N_4)I]\cdot CHCl_3$, space group D_{2h}^{16}-*Pnma* with $a = 8.311$ (1), $b = 13.902$ (3), $c = 21.405$ (5) Å, $Z = 4$; $[Fe(C_{22}H_{22}N_4)Cl]\cdot CH_3CN$, space group C_{2h}^5-$P2_1/c$ with $a = 9.231$ (2), $b = 14.517$ (3), $c = 17.617$ (3) Å, $\beta = 100.10°$, and $Z = 4$; $[Mn(C_{22}H_{22}N_4)(N(C_2H_5)_3)]$, space group C_{2h}^5-$P2_1/c$ with $a = 11.275$ (8), $b = 17.27$ (13), $c = 14.998$ (10) Å, $\beta = 118.50°$, and $Z = 4$. The structures were refined by full-matrix least-squares techniques to conventional R values of 5.2% (2929 data with $F \geq 3\sigma(F)$), 6.4% (5907 data with $F \geq 3\sigma(F)$), and 5.6% (3883 data with $F \geq 3\sigma(F)$) for the Co, Fe, and Mn compounds, respectively. In each structure, the macrocyclic ligand has a pronounced saddle shape due to the steric interactions of the 2,4-pentanediiminato chelate ring methyl groups with the benzenoid rings. The metal is displaced from the macrocyclic N_4 donor plane; the displacement, a function of the metal-N_4 distance, varies from 0.24 Å for the Co(III) complex to 0.730 Å for the Mn(II) complex. The metal nitrogen distances vary from 1.901 Å for the Co(III) complex to 2.118 Å for the Mn(II) complex. The nature of the ligand distortions resulting from ligand steric interactions and the widely varying metal ion radii are presented along with comparisons drawn from closely related tetraphenylporphyrin structures.

The study of the crystal and molecular structures of transition metal complexes, especially those of synthetic and naturally occurring macrocyclic ligands, is necessary to fully understand their physical and chemical properties. The constraints placed on completely conjugated macrocyclic ring systems with respect to radial expansion and contraction of the N_4 donor core, together with the steric requirements of metal ions with varying radii, may lead to unusual coordination geometries and high reactivity.[2,8] Very flat, highly conjugated, four-coordinate macrocyclic complexes may have solid-state intermolecular interactions similar to those of four-coordinate dimethyl glyoxime complexes of Ni(II) and related complexes that become important in determining their physical and chemical properties.[3]

During a series of studies of the complexes of the 7,16-dihydro - 6,8,15,17 - tetramethyldibenzo[*b*,*i*][1,4,8,11]tetraazacyclotetradecinato ligand (I), the macrocyclic ligand obtained by the nickel(II) template condensation of *o*-phenylenediamine with 2,4-pentanedione first described by Jäger,[4] a number of four-,[5] five-, and six-coordinate[6] complexes of divalent and trivalent transition metals with various ground-state electronic configurations were isolated and characterized.

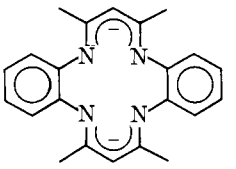

I

The three complexes chosen for this study, $[Co(C_{22}H_{22}N_4)I]\cdot CHCl_3$, $[Fe(C_{22}H_{22}N_4)Cl]\cdot CH_3CN$, and $[Mn(C_{22}H_{22}N_4)N(C_2H_5)_3]$, are five-coordinate. This is an uncommon coordination number for Fe(III) and Mn(II), and especially rare for Co(III) complexes coordinated to nitrogen and halogen ligands. The Fe(III)[6a] and Mn(II)[7] complexes have normal high-spin, $S = 5/2$, configurations, while the Co(III) complex has a rare intermediate $S = 1$ ground state with $\mu_{eff} = 2.80\ \mu_B$.[8] The normal metal-nitrogen distances for these three metal ions having the ground-state configurations specified span a significant range, from about 1.90 Å for Co(III)[9] to approximately 2.27 Å for Mn(II).[10]

The ideal nitrogen-to-center (N-Ct) distance in the neutral ligand, $C_{22}H_{24}N_4$, is 1.902 Å.[5] The loss of two N-H hydrogens

Table I. Crystal Data for $[Mn(C_{22}H_{22}N_4)N(C_2H_5)_3]$, $[Fe(C_{22}H_{22}N_4)Cl]\cdot CH_3CN$, and $[Co(C_{22}H_{22}N_4)I]\cdot CHCl_3$

	$[Mn(C_{22}H_{22}N_4)N(C_2H_5)_3]$	$[Fe(C_{22}H_{22}N_4)Cl]\cdot CH_3CN$	$[Co(C_{22}H_{22}N_4)I]\cdot CHCl_3$
Molecular weight	498.58	474.80	647.66
Space group	$P2_1/c$	$P2_1/c$	*Pnma*
Cell constants			
a, Å	11.275 (8)	9.231 (2)	8.311 (1)
b, Å	17.727 (13)	14.517 (3)	13.902 (3)
c, Å	14.998 (10)	17.617 (3)	21.405 (5)
α, deg	90.0 (0)	90.0 (0)	90.0 (0)
β, deg	118.50 (4)	100.10 (2)	90.0 (0)
γ, deg	90.0 (0)	90.0 (0)	90.0 (0)
No. of reflections used to determine cell constants and their 2θ limits, deg	22 $20 < 2\theta < 40$	28 $37 < 2\theta < 50$	30 $40 < 2\theta < 50$
Z	4	4	4
ρ_{calcd}, g/cm^3	1.257	1.357	1.739
ρ_{expt}, g/cm^3	1.26	1.350	1.74
Absorption coefficients, cm^{-1}	5.84	8.02	23.25
Crystal dimensions, mm	See text	0.35 × 0.35 × 0.25	0.50 × 0.18 × 0.30
Absorption correction	No	No	Yes[a]

[a] Numerical methods employing Ibers' AGNOST program were used to correct intensity data for effects of x-ray absorption.

during the formation of the dianionic ligand and accompanying delocalization probably leads to an even shorter N-Ct distance, which is expected to be in the range from 1.85 to 1.87 Å. Thus, the ideal M-N distance for this dibenzotetraaza[14]annulene ligand is significantly shorter than the porphyrin ligand N-Ct distance, which is about 2.01 Å.[11]

The crystal and molecular structures of these three complexes were determined to systematize the parameters associated with the five-coordinate complexes of the $C_{22}H_{22}N_4^{2-}$ ligand. Another major objective was to evaluate the consequences of the steric interactions occurring on the periphery of the macrocyclic ligand on (a) the structure of the ligand, (b) the coordination geometry of the complex, and (c) the effects of the distortions on the reactivity of the complexes. The axial ligands for all three complexes are weak-field ligands and were expected to have negligible effect on the bond parameters of the macrocyclic moieties. Finally, the possibility of the lattice $CHCl_3$ of the Co(III) compound and the lattice CH_3CN of the Fe(III) having a significant interaction with the complex species in the solid state needed to be explored.[7,12]

Experimental Section

Syntheses. All complexes were prepared under an inert atmosphere.

$[Co(C_{22}H_{22}N_4)I]\cdot CHCl_3$. The free ligand was obtained as previously described.[13] Four-coordinate $[Co(C_{22}H_{22}N_4)]$ was prepared by the reaction of 1 equiv of $C_{22}H_{24}N_4$ dissolved in CH_3CN with 1 equiv of $Co(OAc)_2\cdot 4H_2O$ dissolved in CH_3OH under N_2. A solution containing 100 mg of $[Co(C_{22}H_{22}N_4)]$ in chloroform and a solution of 1.25 ml of 0.1 M I_2 in chloroform were mixed with vigorous agitation at room temperature. The intensely colored purple product which crystallized was filtered under nitrogen, washed with chloroform–diethyl ether mixture, and dried in vacuo: yield, 80%.

Anal. Calcd for $CoC_{23}H_{23}Cl_3IN_4$: C, 42.65; H, 3.58; N, 8.65; Co, 9.37. Found: C, 42.92; H, 3.80; N, 9.09; Co, 9.10.

$[Fe(C_{22}H_{22}N_4)Cl]\cdot CH_3CN$. An acetonitrile solution containing 1 equiv of the free ligand $C_{22}H_{24}N_4$ was added to 1 equiv of tris(*o*-phenylenediamine)iron(II) perchlorate dissolved in CH_3CN. The weakly basic *o*-phenylenediamine deprotonates the macrocyclic ligand. Although an immediate darkening of the solution is noted upon mixing the reagents, the solutions must be allowed to stand for several hours before an appreciable amount of the product crystallizes. The slow crystal growth is facilitated by a slow redox reaction between the proposed iron(II) intermediate complex and the perchlorate anions. In the absence of nonoxidizing anions, a four-coordinate iron(II) complex is isolated. The large black crystals that were isolated had well-formed faces and recrystallization was deemed unnecessary: yield, 38%.

Anal. Calcd for $FeC_{24}H_{25}ClN_5$: C, 60.71; H, 5.27; N, 14.75. Found: C, 60.41; H, 5.47; N, 14.55.

$[Mn(C_{22}H_{22}N_4)N(C_2H_5)_3]$. This complex was prepared by a modification of the procedure reported by Dabrowiak et al.[7] Bis(*o*-phenylenediamine)bisthiocyanatomanganese(II) (1 equiv) and 1 equiv of the free ligand were slurried in acetonitrile followed by the addition of 4 equiv of anhydrous triethylamine. Degassed, anhydrous diethyl ether was introduced dropwise via a syringe through a serum cap until the solution became slightly turbid. The product, which slowly crystallized during a 12-h period, was filtered, washed with a methanol–diethyl ether solution, and dried in vacuo. Both the solutions and the dry crystalline compound are oxygen sensitive. Even in the solid state under inert atmosphere, the complex darkens noticeably with the passage of time (1–2 weeks). All the crystals used for the preliminary crystal examination and data collection were freshly prepared and no more than 2 days had elapsed from sample preparation to data collection.

Anal. Calcd for $MnC_{28}H_{37}N_5$: C, 67.48; H, 7.43; N, 14.00. Found: C, 67.26; H, 7.13; N, 13.75.

Crystal Examination and Data Collection. Precession photographs of crystals of the Fe(III) and Mn(II) complexes showed that they belonged to the monoclinic system. Photographs of the *hk*0, *h*0*l*, and *hkl* reciprocal lattice nets had systematic absences uniquely defining each as belonging to space group C_{2h}^5-$P2_1/c$.[14a] Preliminary precession photographs for the Co(II) complex had symmetry and systematic absences uniquely defining the space groups as *Pnma*.[14b] The refined cell constants and other pertinent crystal data for the three complexes are listed in Table I.

Intensity data were collected by the θ–2θ scan technique on a Picker FACS-1 automated diffractometer.[15] The routine aspects of the data collection details are presented in Table II. The unstable nature of the manganese complex presented difficulties. Substantial crystal decomposition occurred during even short term storage and was accelerated by exposure to x-rays. The first crystal was mounted in a capillary and sealed under nitrogen prior to the initiation of the data collection process. Within a short period of time after the data collection had begun, it became apparent from examination of the standard reflections that crystal decomposition was occurring. Approximately one-third of the way through the data collection, the intensity of the standard reflections had decreased to 85–90% of their original value and the data collection was interrupted. Another crystal from the same batch was mounted and examined, but a comparison of intensity ratios of equivalent reflections collected from the first crystal indicated that the second crystal had already undergone appreciable decomposition. A freshly grown crystal was then mounted, covered with several coats of epoxy resin, and the data collection was continued. The rate of crystal decomposition for the epoxy covered

Table II. Data Collection and Refinement Details for $[Mn(C_{22}H_{22}N_4)N(C_2H_5)_3]$, $[Fe(C_{22}H_{22}N_4)Cl]\cdot CH_3CN$, and $Co(C_{22}H_{22}N_4)]\cdot CHCl_3$

	$[Mn(C_{22}H_{22}N_4)N(C_2H_5)_3]$	$[Fe(C_{22}H_{22}N_4)Cl]\cdot CH_3CN$	$[Co(C_{22}H_{22}N_4)]\cdot CHCl_3$
Diffractometer	Picker FACS-1	Picker FACS-1	Picker FACS-1
Monochrometer (Bragg angle)	Graphite (6.093°)	Graphite (6.093°)	Graphite (6.093°)
Radiation	Mo Kα (0.7107 Å)	Mo Kα (0.7107 Å)	Mo Kα (0.7107 Å)
Takeoff angle, deg	3.0	3.0	3.0
Method	θ–2θ	θ–2θ	θ–2θ
Scan speed	2°/min	2°/min	2°/min
Scan width, deg[a]	2.0	2.0	1.5
Background	20 × 2	20 × 2	20 × 2
Standards	3	3	3
Av max deviations of stds	See text	5%	4%
2θ limits of data, deg	$0 < 2\theta < 50$	$0 < 2\theta < 65$	$0 < 2\theta < 60$
No. of data collected	5248	9144	4112
No. of data used in final refinement	3883 ($F \geq 3\sigma(F)$)	5907 ($F \geq 3\sigma(F)$)	2929 ($F \geq 3\sigma(F)$)
Final R_1 and R_2 (%)[b]	$R_1 = 5.6$; $R_2 = 5.9$	$R_1 = 6.4$; $R_2 = 4.7$	$R_1 = 5.2$; $R_2 = 5.0$
No. of variables (data/variable)	295 (13)	280 (21)	154 (19)

[a] Basic scan width at $2\theta = 0°$; a dispersion factor of 0.692 was used to alter the scan width at higher 2θ values to account for the separation of α_1 and α_2 components. [b] $R_1 = \sum \| F_{obsd} | - | F_{calcd} \| / \sum | F_{obsd} |$; $R_2 = [\sum w(|F_{obsd}| - |F_{calcd}|)^2 / w|F_{obsd}|^2]^{1/2}$.

crystal was comparable to that of the capillary mounted crystals and was the method of choice for protecting the crystals used to complete the data set. A total of four crystals were used during the data collection. Because of the excessive difficulty of producing high quality x-ray crystals on demand, the data collection was terminated at $2\theta = 50°$ rather than our usual 55°. The net intensities from the individual crystals were scaled via the standard reflections to accommodate the variations in crystal size and to account for the intensity falloff that occurred during the data collection.

Relative intensities of the data for the three structures were calculated by

$$I_{rel} = I_{obsd} - [(B_1 + B_2)T]/2t$$

where B_1 and B_2 are the two background counts, T and t are the total scan time and individual background counting time, respectively. Observed structure factors were calculated by using Azaroff's formula for the Lorentz and polarization factors (Lp) under the condition of monochromatized radiation.[16] The standard deviations in I_{rel} and F_{obsd} are estimated by

$$\sigma(I_{rel}) = [I_{obsd} + (T/t)^2(B_1 + B_2) + p_1^2\{I_{obsd} + (T/t)(B_1 + B_2)\}^2]^{1/2}$$

and $\sigma(F_o) = [(I_{rel} + \sigma(I_{rel}))/(Lp)]^{1/2} - (I_{rel}/(Lp))^{1/2}$, where p_1 is a factor, taken here to be 0.02, to account for machine fluctuations and other sources of error which would be expected to result in variations proportional to the diffracted intensity.[17]

Solution and Refinement of the Structures. The structures were solved by standard heavy-atom methods and refined by full-matrix least-squares techniques.[18,19] The initial assignments of the Fe and Cl positional parameters in the Fe(III) complex were in error due to an ambiguity in the Patterson map and led to a structure with apparent disorder. Reexamination of the Patterson map revealed an alternative assignment of the heavy-atom positions, essentially those of the refined coordinates listed in Table V. Heavy-atom phasing used in conjunction with observed structure factor amplitudes yielded a Fourier map from which all nonhydrogen atoms of the macrocyclic ligand were located. Least-squares refinement using isotropic thermal parameters yielded discrepancy indices of 0.119 and 0.174 for R_1 and R_2, respectively. A difference Fourier map revealed the acetonitrile molecule. The positional and thermal parameters of these atoms were refined and a difference Fourier map then revealed all 25 hydrogen atoms. Phenyl and methyl hydrogen atom positions were calculated assuming C–H distances of 0.95 and 1.00 Å, respectively,[20] with least-squares refinement of the latter fitting the observed coordinates to standard tetrahedral geometry. The final least-squares cycles used 5907 reflections with $F_{obsd} \geq 3\sigma(F_{obsd})$ (280 total variables; data/parameter ratio = 21) and with hydrogen atoms included as fixed contributions. Varying the positional and anisotropic thermal parameters for all nonhydrogen atoms, the model converged to the discrepancy indices $R_1 = 0.064$ and $R_2 = 0.047$. The final difference Fourier map was virtually featureless with the largest residual density of 0.35 e/Å^3 located in the vicinity of the acetonitrile molecule.

The solution and refinement of the Co(III) and Mn(II) structures were straightforward. The iodide and the manganese atoms were located from the Patterson map for the Co(III) and Mn(II) complexes,

Table III. Final Positional Parameters for $[Mn(C_{22}H_{22}N_4)N(C_2H_5)_3]$ with Estimated Standard Deviations in Parentheses

Atom	x	y	z
Mn	−0.20047 (5)	0.10573 (3)	0.17214 (4)
N1	−0.3878 (3)	0.1267 (2)	0.0429 (2)
N2	−0.1653 (3)	0.0162 (2)	0.0942 (2)
N3	−0.1113 (3)	0.0225 (2)	0.2864 (2)
N4	−0.3269 (3)	0.1357 (2)	0.2361 (2)
N5	−0.0564 (3)	0.1995 (2)	0.1889 (2)
C1	−0.4438 (3)	0.0863 (2)	−0.0422 (3)
C2	−0.3776 (4)	0.0257 (2)	−0.0598 (3)
C3	−0.2538 (4)	−0.0101 (2)	0.0036 (3)
C4	−0.0442 (3)	−0.0182 (2)	0.1638 (3)
C5	0.0559 (4)	−0.0452 (2)	0.1416 (3)
C6	0.1801 (4)	−0.0678 (2)	0.2174 (4)
C7	0.2086 (4)	−0.0640 (2)	0.3173 (3)
C8	0.1127 (4)	−0.0371 (2)	0.3425 (3)
C9	−0.0141 (4)	−0.0147 (2)	0.2675 (3)
C10	−0.1573 (3)	−0.0017 (2)	0.3474 (2)
C11	−0.2593 (4)	0.0359 (2)	0.3590 (2)
C12	−0.3425 (3)	0.0965 (2)	0.3052 (2)
C13	−0.4145 (4)	0.1921 (2)	0.1729 (3)
C14	−0.4547 (4)	0.2557 (2)	0.2058 (3)
C15	−0.5282 (4)	0.3125 (3)	0.1399 (4)
C16	−0.5602 (4)	0.3080 (3)	0.0395 (4)
C17	−0.5194 (4)	0.2466 (2)	0.0043 (3)
C18	−0.4474 (3)	0.1875 (2)	0.0684 (3)
C19	−0.5882 (4)	0.1002 (3)	−0.1244 (3)
C20	−0.2311 (4)	−0.0852 (2)	−0.0342 (3)
C21	−0.1088 (4)	−0.0755 (2)	0.4043 (3)
C22	−0.4590 (4)	0.1114 (3)	0.3265 (3)
C23	0.0701 (4)	0.1665 (2)	0.1991 (3)
C24	0.1806 (4)	0.2210 (3)	0.2107 (4)
C25	−0.1231 (4)	0.2487 (2)	0.0979 (4)
C26	−0.1533 (5)	0.2125 (3)	−0.0005 (4)
C27	−0.0328 (5)	0.2457 (2)	0.2785 (4)
C28	0.0362 (4)	0.2045 (3)	0.3775 (4)

Table IV. Final Anisotropic Thermal Parameters for $[Mn(C_{22}H_{22}N_4)N(C_2H_5)_3]$ with Estimated Standard Deviations in Parentheses[a]

Atom	β_{11}	β_{22}	β_{33}	β_{12}	β_{13}	β_{23}
Mn	0.00741 (6)	0.00262 (2)	0.00448 (4)	−0.00031 (3)	0.00258 (4)	−0.00027 (2)
N1	0.0065 (3)	0.0032 (1)	0.0035 (1)	−0.0005 (2)	0.0017 (2)	0.0000 (1)
N2	0.0096 (4)	0.0023 (1)	0.0041 (2)	−0.0004 (2)	0.0034 (2)	−0.0004 (1)
N3	0.0087 (3)	0.0025 (1)	0.0038 (2)	0.0004 (2)	0.0025 (2)	−0.0001 (1)
N4	0.0069 (3)	0.0035 (1)	0.0036 (2)	0.0007 (2)	0.00223 (2)	−0.0002 (1)
N5	0.0081 (3)	0.0024 (1)	0.0061 (2)	−0.0002 (2)	0.0033 (2)	−0.0004 (1)
C1	0.0080 (4)	0.0036 (2)	0.0034 (2)	−0.0013 (2)	0.0025 (3)	0.0004 (1)
C2	0.0101 (5)	0.0036 (2)	0.0035 (2)	−0.0015 (2)	0.0030 (3)	−0.0006 (2)
C3	0.0110 (5)	0.0028 (1)	0.0048 (2)	−0.0016 (2)	0.0051 (3)	−0.0007 (1)
C4	0.0090 (4)	0.0018 (1)	0.0051 (2)	−0.0006 (2)	0.0034 (3)	−0.0002 (1)
C5	0.0124 (5)	0.0026 (1)	0.0066 (3)	−0.0003 (2)	0.0060 (3)	0.0001 (2)
C6	0.0111 (5)	0.0034 (2)	0.0093 (4)	0.0008 (2)	0.0067 (4)	0.0006 (2)
C7	0.0090 (5)	0.0036 (2)	0.0086 (4)	0.0007 (2)	0.0036 (3)	0.0008 (2)
C8	0.0097 (5)	0.0034 (2)	0.0054 (3)	0.0005 (2)	0.0030 (3)	0.0002 (2)
C9	0.0088 (5)	0.0019 (1)	0.0052 (3)	−0.0001 (2)	0.0032 (3)	−0.0001 (2)
C10	0.0083 (4)	0.0025 (1)	0.0032 (2)	−0.0003 (2)	0.0011 (3)	−0.0004 (1)
C11	0.0091 (4)	0.0038 (2)	0.0032 (2)	0.0002 (2)	0.0027 (2)	−0.0001 (1)
C12	0.0076 (4)	0.0039 (2)	0.0036 (2)	0.0003 (2)	0.0020 (2)	−0.0009 (2)
C13	0.0054 (4)	0.0034 (1)	0.0049 (2)	0.0001 (2)	0.0022 (3)	0.0000 (2)
C14	0.0083 (5)	0.0045 (2)	0.0059 (3)	0.0008 (2)	0.0032 (3)	−0.0006 (2)
C15	0.0110 (5)	0.0038 (2)	0.0093 (4)	0.0019 (3)	0.0047 (4)	−0.0001 (2)
C16	0.0090 (5)	0.0039 (2)	0.0090 (4)	0.0012 (2)	0.0036 (4)	0.0014 (2)
C17	0.0080 (4)	0.0038 (2)	0.0062 (3)	−0.0001 (2)	0.0027 (3)	0.0009 (2)
C18	0.0052 (5)	0.0031 (1)	0.0048 (3)	−0.0007 (2)	0.0018 (3)	0.0001 (2)
C19	0.0088 (4)	0.0050 (2)	0.0041 (2)	−0.0015 (2)	0.0013 (3)	0.0001 (2)
C20	0.0137 (5)	0.0037 (2)	0.0070 (3)	−0.0019 (2)	0.0060 (4)	−0.0022 (2)
C21	0.0123 (5)	0.0032 (2)	0.0062 (3)	−0.0002 (2)	0.0040 (3)	0.0006 (2)
C22	0.0122 (5)	0.0054 (2)	0.0066 (2)	0.0019 (3)	0.0058 (3)	0.0006 (2)
C23	0.0084 (5)	0.0029 (2)	0.0080 (3)	0.0000 (2)	0.0041 (3)	−0.0007 (2)
C24	0.0092 (5)	0.0039 (2)	0.0136 (4)	−0.0007 (2)	0.0062 (4)	−0.0008 (2)
C25	0.0096 (5)	0.0032 (2)	0.0110 (4)	−0.0009 (2)	0.0038 (4)	0.0014 (2)
C26	0.0149 (7)	0.0088 (3)	0.0078 (4)	−0.0034 (4)	0.0041 (4)	0.0024 (3)
C27	0.0129 (6)	0.0033 (2)	0.0108 (4)	−0.0011 (2)	0.0063 (4)	−0.0024 (2)
C28	0.0173 (7)	0.0070 (3)	0.0068 (3)	−0.0023 (4)	0.0042 (4)	−0.0032 (3)

[a] Anisotropic thermal parameters are of the form $\exp[-(h^2\beta_{11} + k^2\beta_{22} + l^2\beta_{33} + 2hk\beta_{12} + 2hl\beta_{13} + 2kl\beta_{23})]$.

respectively; Fourier syntheses based upon the phases generated by the heavy atoms revealed the positions of the nonhydrogen atoms of the macrocyclic ligand. Fourier and least-squares refinement were used to obtain the coordinates of the remaining nonhydrogen atoms. After refinement of the positional and anisotropic thermal parameters for the heavy atoms and the positional and isotropic thermal parameters for the nonhydrogen atoms, difference Fourier maps were obtained to locate trial coordinates for the methyl hydrogen atoms, while the coordinates for all other hydrogen atoms were calculated. The contributions from the hydrogen atoms were included as fixed contributions in the final refinements. The final cycles of full-matrix least-squares refinement varied the positional and anisotropic thermal parameters for all nonhydrogen atoms. The final agreement indices are given in Table II. Final difference maps were generally featureless except for a peak of 0.7 e/Å^3 in the vicinity of a chlorine atom (Cl2) of the chloroform in the Co(III) structure and a peak of 0.4 e/Å^3 near one of the ethyl groups of the triethylamine in the Mn(II) structure. The final positional and thermal parameters, along with their estimated standard deviations for the structures are listed in Tables III–VIII. Listings of the derived hydrogen atom coordinates and the observed and calculated structure factors are available.[21]

Results and Discussion of the Structures

General. The structure of each compound reveals a five-coordinate complex with the metal bound to the four nitrogen atoms of the macrocyclic ligand and weakly bound to a fifth axial ligand. The fifth coordination sitecontains an iodide anion, a chloride anion, and a molecule of triethylamine for Co(III), Fe(III), and Mn(II) complexes, respectively. The Co(III) and the Fe(III) structures contain solvent molecules trapped in lattice cavities formed by the packing of the large complex molecules. There is no significant interaction of the solvent molecules with the vacant coordination sites or with the ligand. In all three structures the macrocyclic ligand has a pronounced saddle shape, which is primarily attributable to the steric interactions of the methyl groups derived from the 2,4-pentanediiminato linkages with the benzenoid rings. The degree of warping of the ligand is also strongly influenced by the size of the metal ion; the maximum distortion is found in the Mn(II) complex, the minimum in the Co(III) complex.

Views of the Co(III), Mn(II), and Fe(III) complexes, approximately normal to the plane of the macrocyclic ligand, together with the labeling scheme and selected interatomic distances of the macrocyclic ligand are shown in Figures 1 through 3. Perspectives of each molecule from the side illustrating the saddle shape of the macrocyclic ligand and the inner coordination sphere are presented in Figures 4 through 6. The packing of the complexes and solvent molecules in the unit cells is shown in Figures 7 through 9. A summary of the more important bond angles is presented in Tables IX through XI. To fully understand the details of the inner coordination sphere of these complexes, it is first necessary to examine the nature of the macrocyclic ligand and the structural aspects of the ligand in each complex.

The Macrocyclic Ligand. The macrocyclic ligand is a tetramethylated derivative of the dibenzotetraaza[14]annulene ligand. The ligand is dianionic, thus the inner 14-membered macrocyclic ring of the ligand is ostensibly a 16 π-electron system. The patterns of bond lengths in each of the macrocyclic ligands are clearly not those of an aromatic macroring system. The chemically equivalent bond distances of the macrocyclic ligand in each complex are almost identical within the estimated standard deviations. Each structure contains fully delocalized 2,4-pentanediminato chelate rings separated from

Table V. Final Atomic Coordinates for $[Fe(C_{22}H_{22}N_4)]\cdot CH_3CN$ with Estimated Standard Deviations in Parentheses

Atom	x	y	z
Fe	0.0985 (1)	0.2422 (1)	−0.0431 (1)
Cl	−0.0219 (1)	0.2486 (1)	0.0573 (1)
N1	0.3133 (2)	0.2276 (1)	−0.0003 (1)
N4	0.1272 (2)	0.1095 (1)	−0.0685 (1)
N3	−0.0536 (2)	0.2527 (1)	−0.1383 (1)
N2	0.1325 (2)	0.3727 (1)	−0.0724 (1)
C1	0.4224 (3)	0.2853 (2)	−0.0074 (1)
C2	0.3952 (3)	0.3739 (2)	−0.0382 (2)
C3	0.2612 (3)	0.4163 (2)	−0.0685 (1)
C4	−0.0079 (3)	0.4103 (2)	−0.1034 (1)
C5	−0.0557 (3)	0.5005 (2)	−0.0954 (2)
C6	−0.2004 (3)	0.5247 (2)	−0.1223 (2)
C7	−0.3007 (3)	0.4589 (2)	−0.1548 (2)
C8	−0.2574 (3)	0.3688 (2)	−0.1620 (2)
C9	−0.1108 (3)	0.3436 (2)	−0.1383 (1)
C10	−0.0844 (3)	0.1936 (2)	−0.1966 (1)
C11	−0.0208 (3)	0.1059 (2)	−0.1929 (2)
C12	0.0796 (3)	0.0649 (2)	−0.1337 (2)
C13	0.2275 (3)	0.0728 (2)	−0.0051 (1)
C14	0.2216 (3)	−0.0147 (2)	0.0261 (2)
C15	0.3204 (3)	−0.0390 (2)	0.0912 (2)
C16	0.4228 (3)	0.0233 (2)	0.1266 (2)
C17	0.4272 (3)	0.1119 (2)	0.0978 (2)
C18	0.3316 (3)	0.1377 (2)	0.0319 (1)
C19	0.5817 (3)	0.2570 (2)	0.0138 (2)
C20	0.2706 (3)	0.5112 (2)	−0.1008 (2)
C21	−0.1830 (3)	0.2192 (2)	−0.2708 (2)
C22	0.1361 (3)	−0.0287 (2)	−0.1495 (2)
C23	0.2372 (5)	0.2079 (4)	0.2442 (2)
C24	0.3584 (7)	0.2705 (4)	0.2524 (3)
N5	0.4510 (6)	0.3178 (4)	0.2569 (3)

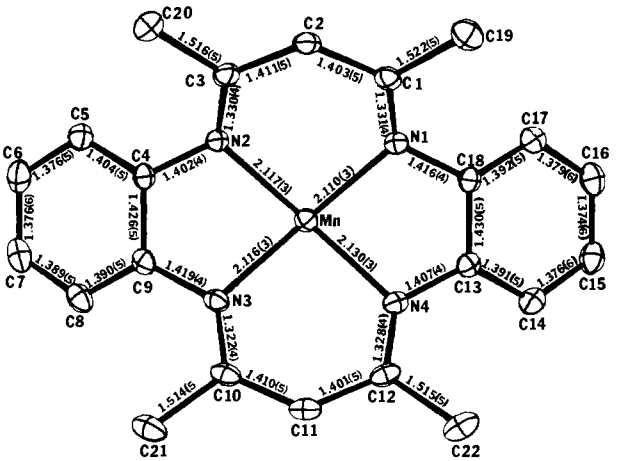

Figure 1. Projection down the Mn–N bond axis of $[Mn(C_{22}H_{22}N_4)\text{-}N(C_2H_5)_3]$ illustrating the labeling scheme and the interatomic distances within the ligand and the coordination sphere. The triethylamine has been omitted for clarity of presentation. The thermal ellipsoids are drawn at the 20% probability level.

aromatic benzenoid rings by nominal single C–N bonds in the five-membered chelate rings. The average of the C–N bond lengths which link the two delocalized systems together is 1.414 Å for the three structures and contains the greatest amount of single bond character. The lack of delocalization between the benzenoid rings and the 2,4-pentanediiminato rings is not attributable to the large torsional angles about the C–N linkages (vide infra), but is a consequence of the stability inherent in the aromatic benzene rings and the quasiaromatic 2,4-pentanediiminato chelate rings.[22,23]

Table VI. Final Anisotropic Thermal Parameters for $[Fe(C_{22}H_{22}N_4)Cl]\cdot CH_3CN$ with Estimated Standard Deviations in Parentheses[a]

	β_{11}	β_{22}	β_{33}	β_{12}	β_{13}	β_{23}
Fe	0.0086 (1)	0.0024 (1)	0.0026 (1)	−0.0003 (1)	−0.0000 (1)	−0.0000 (1)
Cl	0.0129 (1)	0.0043 (1)	0.0030 (1)	−0.0001 (1)	0.0019 (1)	0.0000 (1)
N1	0.0080 (3)	0.0028 (1)	0.0027 (1)	−0.0000 (1)	0.0002 (1)	0.0000 (1)
N4	0.0095 (3)	0.0024 (1)	0.0027 (1)	−0.0006 (1)	0.0010 (1)	−0.0002 (1)
N3	0.0091 (3)	0.0030 (1)	0.0021 (1)	−0.0005 (2)	0.0002 (1)	−0.0003 (1)
N2	0.0089 (3)	0.0025 (1)	0.0022 (1)	−0.0004 (1)	−0.0000 (1)	0.0000 (1)
C1	0.0075 (4)	0.0032 (1)	0.0028 (1)	−0.0005 (2)	−0.0000 (2)	−0.0002 (1)
C2	0.0086 (4)	0.0034 (1)	0.0034 (1)	−0.0019 (2)	0.0002 (2)	0.0001 (1)
C3	0.0115 (4)	0.0028 (1)	0.0025 (1)	−0.0012 (2)	−0.0000 (2)	0.0000 (1)
C4	0.0099 (3)	0.0030 (1)	0.0019 (1)	0.0000 (2)	0.0001 (2)	0.0000 (1)
C5	0.0129 (4)	0.0032 (1)	0.0025 (1)	0.0008 (2)	−0.0000 (2)	0.0000 (1)
C6	0.0159 (5)	0.0042 (2)	0.0031 (1)	0.0033 (2)	0.0008 (2)	0.0002 (1)
C7	0.0105 (5)	0.0065 (2)	0.0032 (1)	0.0029 (2)	0.0004 (2)	0.0007 (1)
C8	0.0093 (4)	0.0051 (2)	0.0028 (1)	−0.0002 (2)	−0.0000 (2)	0.0001 (1)
C9	0.0092 (3)	0.0034 (1)	0.0018 (1)	−0.0001 (2)	0.0002 (1)	0.0001 (1)
C10	0.0110 (4)	0.0037 (1)	0.0020 (1)	−0.0018 (2)	0.0005 (2)	−0.0002 (1)
C11	0.0133 (4)	0.0034 (1)	0.0025 (1)	−0.0022 (2)	0.0007 (2)	−0.0011 (1)
C12	0.0119 (4)	0.0026 (1)	0.0031 (1)	−0.0016 (2)	0.0023 (2)	−0.0004 (1)
C13	0.0100 (3)	0.0027 (1)	0.0029 (1)	0.0007 (2)	0.0016 (1)	−0.0000 (1)
C14	0.0134 (4)	0.0028 (2)	0.0041 (1)	−0.0001 (2)	0.0023 (2)	0.0001 (1)
C15	0.0171 (5)	0.0034 (2)	0.0043 (1)	0.0020 (2)	0.0025 (2)	0.0016 (1)
C16	0.0149 (5)	0.0051 (2)	0.0035 (1)	0.0026 (2)	0.0005 (2)	0.0013 (1)
C17	0.0116 (4)	0.0046 (2)	0.0033 (1)	0.0006 (1)	0.0001 (2)	0.0003 (1)
C18	0.0090 (3)	0.0030 (1)	0.0028 (1)	0.0004 (2)	0.0012 (1)	0.0002 (1)
C19	0.0090 (4)	0.0048 (2)	0.0050 (1)	−0.0005 (2)	0.0006 (2)	0.0004 (1)
C20	0.0125 (5)	0.0039 (2)	0.0059 (1)	−0.0020 (3)	−0.0003 (2)	0.0015 (1)
C21	0.0162 (4)	0.0046 (2)	0.0024 (1)	−0.0016 (2)	−0.0002 (2)	−0.0004 (1)
C22	0.0213 (5)	0.0036 (2)	0.0039 (1)	0.0001 (3)	0.0022 (2)	−0.0012 (1)
C23	0.0294 (9)	0.0192 (5)	0.0045 (2)	0.0109 (5)	0.0049 (3)	0.0023 (2)
C24	0.0147 (12)	0.0128 (5)	0.0091 (3)	0.0065 (5)	−0.0021 (5)	−0.0020 (3)
N5	0.0251 (14)	0.0148 (6)	0.0208 (3)	0.0033 (6)	−0.0028 (6)	−0.0045 (3)

[a] Anisotropic thermal parameters are of the form $\exp[-(h^2\beta_{11} + k^2\beta_{22} + l^2\beta_{33} + 2hk\beta_{12} + 2hl\beta_{13} + 2kl\beta_{23})]$.

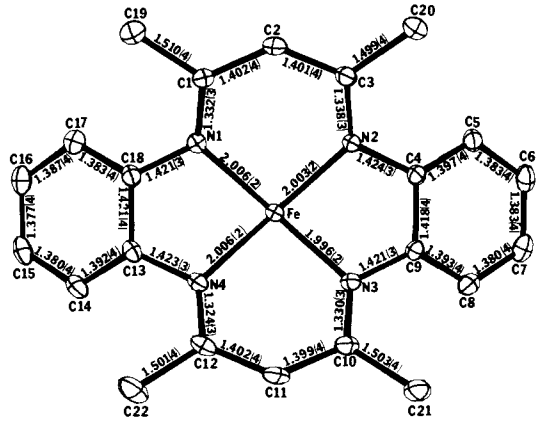

Figure 2. Projection down the Fe–Cl bond axis of $[Fe(C_{22}H_{22}N_4)Cl]$ illustrating the labeling scheme and the interatomic distances within the ligand and the coordination sphere. The chloride ion has been omitted for clarity of presentation. The vibrational ellipsoids are drawn at the 20% probability level.

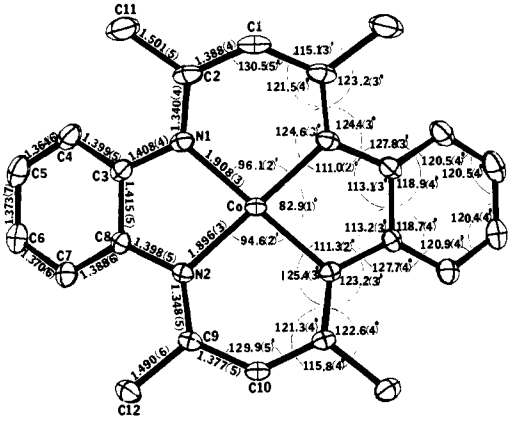

Figure 3. Projection of $[Co(C_{22}H_{22}N_4)I]$ down the Co–I bond axis with the labeling scheme and selected interatomic distance and angles. The vibrational ellipsoids are drawn at the 20% probability level.

Table VII. Final Atomic Positional Parameters for $[Co(C_{22}H_{22}N_4)I]\cdot CHCl_3$ with Estimated Standard Deviations in Parentheses

Atom	x	y	z
I	0.21639 (5)	0.25000	0.06785 (2)
Co	−0.03870 (8)	0.25000	0.13455 (3)
N1	−0.1427 (4)	0.1479 (2)	0.0908 (1)
N2	0.0181 (4)	0.1498 (2)	0.1905 (1)
C1	−0.3237 (6)	0.2500	0.0358 (2)
C2	−0.2682 (4)	0.1593 (3)	0.0522 (1)
C3	−0.0708 (4)	0.0588 (3)	0.1047 (2)
C4	−0.0708 (5)	−0.0248 (3)	0.0683 (2)
C5	0.0204 (6)	−0.1022 (3)	0.0851 (2)
C6	0.1137 (6)	−0.0993 (4)	0.1380 (3)
C7	0.1169 (6)	−0.0184 (3)	0.1745 (2)
C8	0.0220 (5)	0.0608 (3)	0.1601 (2)
C9	0.0447 (5)	0.1603 (3)	0.2522 (2)
C10	0.0544 (8)	0.2500	0.2792 (3)
C11	−0.3668 (5)	0.0769 (3)	0.0280 (2)
C12	0.0481 (6)	0.0773 (4)	0.2963 (2)
C13	0.1861 (9)	−0.2500	0.3528 (4)
Cl1	0.2808 (4)	−0.25000	0.2852 (1)
Cl2	0.0652 (3)	−0.1515 (1)	0.3628 (1)

Distortions from Planarity. The side view of each structure reveals a pronounced saddle shape for the macrocyclic ligand. This marked nonplanarity, arising from the steric interactions of the methyl groups with the benzenoid rings, is the most important feature governing the structure and reactivity of these complexes. The differences in the details of the structure of the ligand and the primary coordination sphere are determined by a second factor—the radius of the metal. A third factor of lesser importance influencing the placement of the metal with respect to the N_4 plane is the number and type of ligands occupying the axial sites.[24] The first two aspects will now be examined in detail.

Since most first-row transition metals have M–N distances longer than the ideal 1.85–1.87 Å afforded by this ligand, some mechanism or mechanisms of ligand deformation must exist to accommodate these metals. The three most obvious possibilities are: (1) a slight increase in all of the interatomic distances in the 14-membered ring; (2) an increase in the various interior and exterior angles of the 14-membered ring ($\alpha,\beta,\gamma,\delta$ in Figure 10); and (3) torsional distortions about the appropriate bonds redirecting the N_4 lone pairs out of the N_4 plane.

Table VIII. Final Anisotropic Thermal Parameters for $[Co(C_{22}H_{22}N_4)I]\cdot CHCl_3$ with Estimated Standard Deviations in Parentheses[a]

Atom	β_{11}	β_{22}	β_{33}	β_{12}	β_{13}	β_{23}
I	0.01082 (6)	0.00652 (3)	0.00295 (1)	0.0	0.00130 (2)	0.0
Co	0.00873 (9)	0.00455 (4)	0.00146 (2)	0.0	−0.00043 (3)	0.0
N1	0.0091 (4)	0.0044 (1)	0.0015 (1)	−0.0006 (2)	0.0002 (1)	0.0000 (1)
N2	0.0108 (5)	0.0055 (2)	0.0018 (1)	0.0000 (3)	−0.0008 (2)	0.0004 (1)
C1	0.0093 (8)	0.0056 (3)	0.0016 (1)	0.0	−0.0008 (2)	0.0
C2	0.0095 (5)	0.0052 (2)	0.0014 (1)	−0.0009 (3)	0.0001 (2)	−0.0002 (1)
C3	0.0109 (6)	0.0041 (2)	0.0019 (1)	−0.0004 (3)	0.0007 (2)	0.0004 (1)
C4	0.0155 (7)	0.0051 (2)	0.0022 (1)	−0.0006 (4)	0.0011 (2)	0.0003 (1)
C5	0.0204 (9)	0.0045 (3)	0.0034 (1)	0.0005 (4)	0.0020 (3)	0.0003 (2)
C6	0.0191 (9)	0.0055 (3)	0.0046 (2)	0.0026 (4)	0.0006 (3)	0.0016 (2)
C7	0.0164 (8)	0.0063 (3)	0.0033 (1)	0.0010 (4)	−0.0009 (3)	0.0016 (2)
C8	0.0113 (6)	0.0052 (2)	0.0022 (1)	−0.0003 (3)	−0.0003 (2)	0.0010 (1)
C9	0.0113 (6)	0.0081 (3)	0.0019 (1)	−0.0010 (4)	−0.0014 (2)	0.0007 (2)
C10	0.0157 (10)	0.0096 (5)	0.0015 (1)	0.0	−0.0015 (3)	0.0
C11	0.0144 (7)	0.0059 (3)	0.0024 (1)	−0.0019 (4)	−0.0009 (2)	−0.0004 (1)
C12	0.0241 (10)	0.0103 (4)	0.0024 (1)	−0.0026 (6)	−0.0025 (3)	0.0016 (2)
C13	0.0219 (14)	0.0075 (5)	0.0037 (2)	0.0	−0.0030 (5)	0.0
Cl1	0.0370 (8)	0.0464 (8)	0.0041 (1)	0.0	0.0012 (2)	0.0
Cl2	0.0533 (7)	0.0085 (1)	0.0114 (1)	0.0057 (2)	−0.0071 (2)	−0.0031 (1)

[a] Anisotropic thermal parameters are of the form $\exp[-(h^2\beta_{11} + k^2\beta_{22} + l^2\beta_{33} + 2hk\beta_{12} + 2hl\beta_{13} + 2kl\beta_{23})]$.

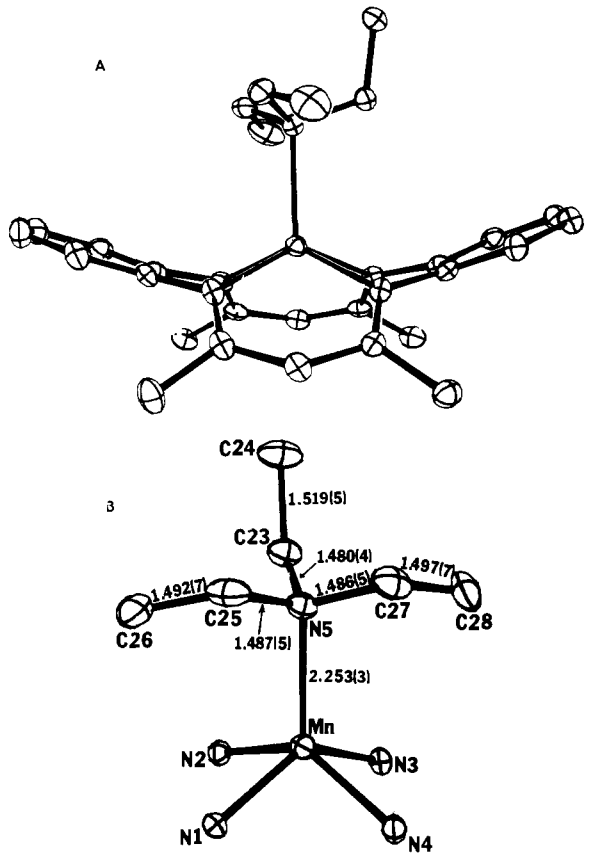

Figure 4. (A) Side view of $[Mn(C_{22}H_{22}N_4)N(C_2H_5)_3]$ illustrating the saddle shape of the ligand and the orientation of the triethylamine ligand. Vibrational ellipsoids are drawn at the 20% probability level. (B) Side view of the inner coordination sphere of $[Mn(C_{22}H_{22}N_4)N(C_2H_5)_3]$ with labeling scheme and the interatomic distances of the triethylamine moiety.

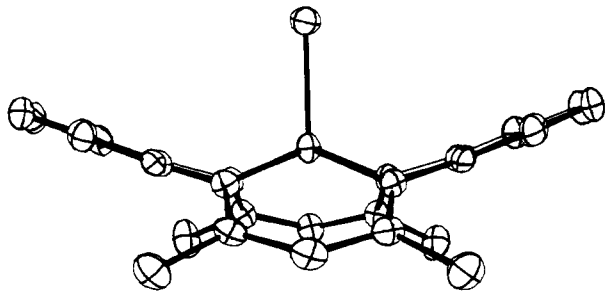

Figure 5. Side view of the $[Fe(C_{22}H_{22}N_4)Cl]$ complex.

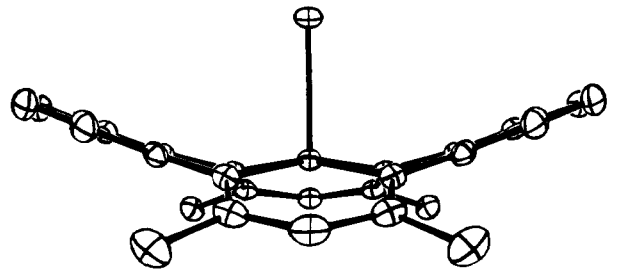

Figure 6. Side view of $[Co(C_{22}H_{22}N_4)I]$.

The last option will displace the metal from the N_4 donor plane and increase the M–N distances without necessarily altering the N–Ct distance.

The strain resulting from the steric interactions and the coordination to a metal can be minimized by distributing the compensation among the three possibilities mentioned. Distortions of bond lengths are energetically expensive and thus likely to be small. The vagaries of lattice energies, estimated standard deviations (esd's), etc., are such that any systematic bond lengthening within the ligand framework to accommodate the metals with larger radii is unobservable. Angle deformations and torsional motions are energetically less costly than bond stretchings, thus factors 2 and 3 are more apt to be observable. A number of important average bond parameters for the three $[M(C_{22}H_{22}N_4)X]$ structures, tabulated in Table XIV, support the latter contentions. For each of the averaged chemically independent angles within the 14-membered rings ($\alpha,\beta,\gamma,\delta$), there is a systematic increase of 1–2° on going from the Co(III) structure (with the smallest metal radius) to the Mn(II) structure (which has the largest radius). The total angular increase of the ten interior and four exterior angles for the entire macrocycle on going from the Co(III) structure to the Mn(II) structure is 28.4° and is sufficient to account for most of the observed increase in the N–Ct distance from 1.893 to 1.988 Å.

As mentioned, the steric interaction of the methyl groups with the benzenoid rings is relieved primarily through deviations of the various torsional angles from their ideal value of 0 or 180°. These distortions occur principally through twisting about the C–N bonds in the five- and six-membered chelate rings. Individual dihedral angles are defined and tabulated in Tables XII and XIII; the chemically averaged values yield some significant trends (see Table XIV and Figure 10). For the cas of the Mn(II) structure the metal ion is much too large to fit in the N_4 plane and a significant amount of torsional action within the macrocycle framework is necessary to redirect the N_4 lone pairs towards the metal. The torsional angles about the C–N bonds of the five-membered chelate rings defined in Table XII are very large, 51.3°. Those involving the C–N bonds in the six-membered chelate rings are small, 1.6°.

However, as the metal descends into the N_4 plane, as in the case of Co(III), whose normal Co–N distances are compatible with the N–Ct distance of the macrocyclic ligand, the N_4 lone pairs must be directed into the N_4 plane, which necessarily results in a decrease of the C–N (five-membered ring) torsional angles. Such a decrease, without any other compensating effects, would increase the contact between the CH_3 and benzenoid groups. To prevent such additional compressional strain, distortions occur at the next most readily deformable site, the torsional angles about the C–N bonds of the 2,4-pentanediiminato rings. These increase from a small angle of 1.6° for the Mn(II) complex to a very substantial 12.1° for the Co(III) complex. As expected, the torsional angles about the various C–N bonds for the Fe(III) complex fall midway between the two extremes, but are closer to those of the Mn(II) structure. The steric strain between the CH_3 groups and the benzenoid rings increases on flattening of the macrocyclic ring as is observed by comparing the closest methyl–benzene contacts in the three structures. The average value decreases from 3.126 Å for the Mn(II) complex to 2.949 Å for the Co(III) complex.

There are small but important trends in the changes of the average C–N and C–C bond lengths within the 2,4-pentanediiminato rings (Table XIV) on going from the Mn(II) complex to the Co(III) complex, which correlate with the magnitude of the dihedral angles involving the C–N bonds. The overlap of the p–π orbitals decreases with increasing twist angle and results in a decrease in the delocalization in the chelate ring. This is accompanied by a redistribution of charge density within the ring, as indicated by a systematic shortening of the C–C bonds, and a dramatic increase in the reactivity at the methine carbon atom.[8]

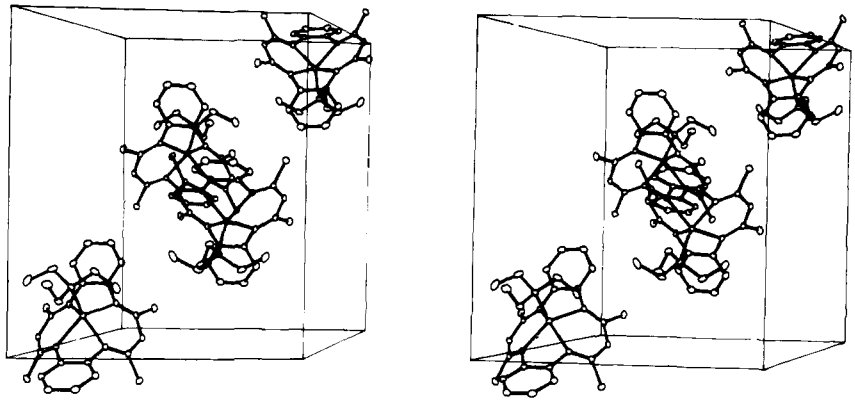

Figure 7. Stereoscopic view of the unit cell contents and packing arrangement of $[Mn(C_{22}H_{22}N_4)N(C_2H_5)_3]$ as viewed down the axis normal to the "*bc*" face.

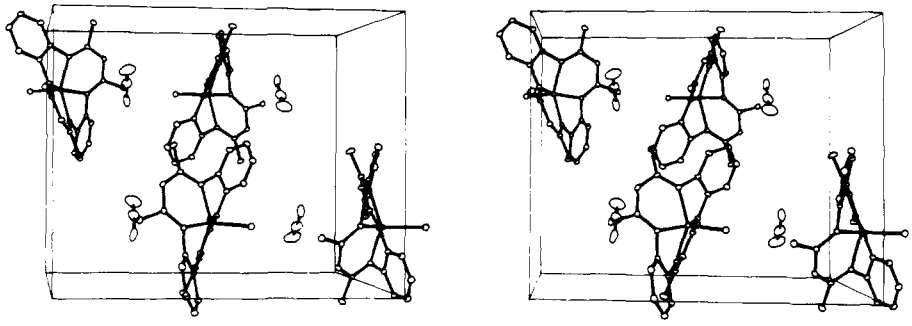

Figure 8. Stereoscopic view, normal to the "*bc*" face illustrating the unit cell contents and packing arrangement of $[Fe(C_{22}H_{22}N_4)Cl]CH_3CN$ and showing the location of the lattice CH_3CN with respect to the packing of the Fe(III) species.

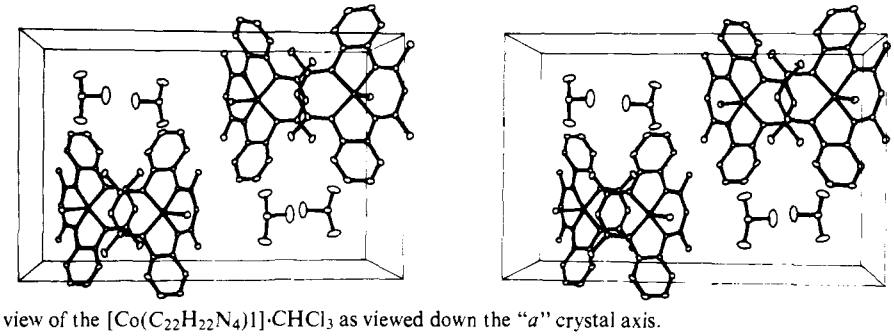

Figure 9. Stereoscopic view of the $[Co(C_{22}H_{22}N_4)I]\cdot CHCl_3$ as viewed down the "*a*" crystal axis.

The twisting about the various bonds just described gives rise to the saddle shape as depicted in Figures 4 through 6. The effects of these twists can best be understood by considering the angles of intersection of the various planes of the chelate rings and benzenoid rings with the N_4 donor plane (see Figure 10). The individual values are given in Table XIII, the average values in Table XIV. For all three complexes, the dihedral angle between the N_4 donor plane (plane 1) and the 2,4-pentanediiminato rings (plane 2) is significantly larger than the dihedral angle between the five-membered chelate rings (plane 3) and the N_4 plane. Thus, for all three complexes the donor pars are directed out of the N_4 plane on the same side of the macrocyclic ligand to which the benzene rings are tipped. This accounts for the fact that the axial ligand of these complexes is always found on the same side of the macrocyclic ligand. The dihedral angles of the N_4 plane with plane 2 vary from 21.31° for the Co(III) complex to 35.20° for the Mn(II) complex. Interestingly, as the dihedral angle of the N_4 plane with plane 2 increases, the dihedral angle with plane 3 decreases, paralleling the elevation of the metal from the N_4 plane (Table XIV).

Inner Coordination Sphere. With the above constraints governing the overall macrocyclic ligand conformation, the details of the inner coordination sphere become readily understood. The inherent predisposition of the $C_{22}H_{22}N_4^{2-}$ ligand to direct the metal out of the N_4 coordination plane leads to nonequivalent axial ligand sites and to a preference for five-coordination.

The metal-N_4 nitrogen distances will be considered first. The average Co(III)-N_4 distance, 1.901 Å, is normal and in the range commonly observed for Co(III)-N distances with unsaturated amine ligands such as dimethyl glyoxime.[9] Although the M-N distances for Co(III) are expected to be a function of the ground-state electronic configuration, the $x^2 - y^2$ orbital is vacant for both $S = 1$ and $S = 0$ configurations and leads to similar M-N for the two ground states. The Fe(III) and Mn(II) complexes have $S = \frac{5}{2}$ ground states, with the $x^2 - y^2$ orbitals occupied, resulting in much larger radii than for Co(III). The radius of Mn(II) is larger than Fe(III) because of Coulombic factors. Thus the Fe(III)-N_4 average distance of 2.002 Å is nearly 0.1 Å longer than for the Co(III) complex and the Mn(II)-N distance is 2.118 Å, 0.217 Å longer than in the Co(III) complex. The Fe-N and Mn-N distances are significantly shorter than normal. Commonly observed high-spin Fe(III)-N and Mn(II)-N distances are 2.15 and 2.25 Å, respectively, thus indicating a substantial bond

Table IX. Bond Angles (deg) for $[Mn(C_{22}H_{22}N_4)N(C_2H_5)_3]$

N1-Mn-N2	89.7 (1)	N2-C3-C20	120.8 (4)
N1-Mn-N4	77.2 (1)	C2-C3-C20	115.6 (3)
N3-Mn-N2	77.4 (1)	N2-C4-C5	125.4 (3)
N3-Mn-N4	88.3 (1)	N2-C4-C9	115.7 (3)
N1-Mn-N3	138.4 (1)	C5-C4-C9	118.2 (3)
N2-Mn-N4	141.0 (1)	C4-C5-C6	121.3 (4)
N1-Mn-N5	109.0 (1)	C5-C6-C7	120.1 (4)
N2-Mn-N5	107.4 (1)	C6-C7-C8	120.4 (4)
N3-Mn-N5	112.6 (1)	C7-C8-C9	120.7 (4)
N4-Mn-N5	111.6 (1)	C8-C9-C4	119.3 (3)
Mn-N1-C1	126.5 (3)	N3-C9-C4	115.7 (3)
Mn-N1-C18	106.4 (2)	N3-C9-C8	124.4 (3)
C1-N1-C18	126.9 (3)	N3-C10-C11	123.0 (3)
Mn-N2-C3	125.5 (2)	N3-C10-C21	121.1 (3)
Mn-N2-C4	106.8 (2)	C11-C10-C21	115.8 (3)
C3-N2-C4	126.6 (3)	C10-C11-C12	130.8 (3)
Mn-N3-C9	106.1 (2)	N4-C12-C11	123.3 (3)
Mn-N3-C10	126.5 (2)	N4-C12-C22	121.6 (3)
C9-N3-C10	125.7 (3)	C11-C12-C12	114.9 (3)
Mn-N4-C12	126.0 (2)	N4-C13-C14	125.4 (3)
Mn-N4-C13	106.2 (2)	N4-C13-C18	115.4 (3)
C12-N4-C13	125.9 (3)	C14-C13-C18	118.5 (3)
Mn-N5-C23	109.1 (2)	C13-C14-C15	121.6 (4)
Mn-N5-C25	108.0 (2)	C14-C15-C16	119.8 (4)
Mn-N5-C27	108.4 (2)	C15-C16-C17	120.3 (4)
C23-N5-C25	111.6 (3)	C16-C17-C18	121.3 (4)
C23-N5-C27	112.2 (3)	C17-C18-C13	118.4 (4)
C25-N5-C27	107.5 (3)	N1-C18-C13	115.5 (3)
N1-C1-C2	122.8 (3)	N1-C18-C17	125.6 (3)
N1-C1-C19	121.6 (4)	N5-C23-C24	117.2 (3)
C2-C1-C19	115.5 (3)	N5-C25-C26	115.6 (4)
C1-C2-C3	131.5 (3)	N5-C27-C28	114.3 (4)
N2-C3-C2	123.3 (3)		

shortening due to the constraints imposed by the macrocycle.

The constraining nature of the macrocyclic ligands prevents the N-Ct distance from lengthening to the ideal M-N distances preferred by Fe(III) and Mn(II). A significant ex-

Table X. Bond Angles (deg) for $[Fe(C_{22}H_{22}N_4)Cl]\cdot CH_3CN$

N1-Fe-C1	107.47 (6)	N2-C4-C5	127.0 (2)
N4-Fe-C1	108.54 (6)	N2-C4-C9	113.6 (2)
N3-Fe-C1	106.63 (6)	C5-C4-C9	119.0 (2)
N2-Fe-C1	106.55 (6)	C4-C5-C6	120.4 (3)
N1-Fe-N4	79.71 (8)	C5-C6-C7	120.2 (3)
N1-Fe-N3	145.90 (8)	C6-C7-C8	120.6 (3)
N1-Fe-N2	90.45 (8)	C7-C8-C9	120.2 (3)
N4-Fe-N3	89.26 (8)	N3-C9-C4	114.4 (2)
N4-Fe-N2	144.91 (8)	N3-C9-C8	125.8 (2)
N3-Fe-N2	80.23 (8)	C4-C9-C8	119.5 (2)
Fe-N1-C1	127.6 (2)	N3-C10-C11	121.4 (2)
Fe-N1-C18	106.7 (2)	N3-C10-C21	121.8 (2)
C1-N1-C18	125.2 (2)	C11-C10-C21	116.8 (2)
Fe-N4-C12	128.8 (2)	C10-C11-C12	129.7 (3)
Fe-N4-C13	106.1 (2)	N4-C12-C11	120.9 (2)
C12-N4-C13	124.7 (2)	N4-C12-C22	122.1 (2)
Fe-N3-C9	106.1 (1)	C11-C12-C22	116.9 (2)
Fe-N3-C10	128.5 (2)	N4-C13-C14	126.0 (2)
C9-N3-C10	124.8 (2)	N4-C13-C18	114.1 (2)
Fe-N2-C3	127.8 (2)	C14-C13-C18	119.6 (2)
Fe-N2-C4	106.7 (1)	C13-C14-C15	119.8 (3)
C3-N2-C4	125.4 (2)	C14-C15-C16	120.6 (3)
N1-C1-C2	121.8 (2)	C15-C16-C17	120.5 (3)
N1-C1-C19	121.6 (2)	C16-C17-C18	120.2 (3)
C2-C1-C19	116.5 (2)	N1-C18-C13	113.6 (2)
C1-C2-C3	129.5 (3)	N1-C18-C17	126.8 (2)
N2-C3-C2	121.9 (2)	C13-C18-C17	119.2 (2)
N2-C3-C20	121.7 (2)	N5-C24-C23	178.3 (8)
C2-C3-C20	116.3 (2)		

Table XI. Bond Angles (deg) for $[Co(C_{22}H_{22}N_4)I]\cdot CHCl_3$

I-Co-N1	95.8 (1)
I-Co-N2	98.4 (1)
N1-Co-N2	89.2 (1)
N1-Co-N1(m)[a]	96.1 (2)
N2-Co-N2(m)	94.6 (2)
Co-N1-C2	124.6 (3)
Co-N1-C3	111.0 (2)
C2-N1-C3	124.4 (3)
Co-N2-C8	111.3 (2)
Co-N2-C9	125.4 (3)
C8-N2-C9	123.2 (3)
C2-C1-C2(m)	130.5 (5)
N1-C2-C1	121.5 (4)
N1-C2-C11	123.2 (3)
C1-C2-C11	115.1 (3)
N1-C3-C4	127.8 (3)
N1-C3-C8	113.1 (3)
C4-C3-C8	118.9 (4)
C3-C4-C5	120.5 (4)
C4-C5-C6	120.5 (4)
C5-C6-C7	120.4 (4)
C6-C7-C8	120.9 (4)
N2-C8-C3	113.2 (3)
N2-C8-C7	127.7 (4)
C3-C8-C7	118.7 (4)
N2-C9-C10	121.3 (4)
N2-C9-C12	122.6 (4)
C10-C9-C12	115.8 (4)
C9-C10-C9(m)	129.9 (5)
Cl1-C13-Cl2	113.0 (3)
Cl2-C13-Cl2(m)	106.2 (5)

[a] The letter "m" denotes those atoms related by the crystallographic mirror plane.

Table XII. Selected Dihedral Angles (deg)

Atoms defining planes	$[Mn(C_{22}H_{22}N_4)N(C_2H_5)_3]$	$[Fe(C_{22}H_{22}N_4)Cl]\cdot CH_3CN$
C17-C18-N1 / C18-N1-C1	45.1 (5)	43.1 (4)
C18-N1-C1 / N1-C1-C19	2.4 (5)	4.4 (4)
C5-C4-N2 / C4-N2-C3	51.0 (5)	39.2 (4)
C4-N2-C3 / N2-C3-C20	1.1 (5)	2.7 (4)
C8-C9-N3 / C9-N3-C10	54.3 (5)	46.2 (4)
C9-N3-C10 / N3-C10-C21	0.7 (5)	1.5 (4)
C14-C13-N4 / C13-N4-C12	54.8 (5)	45.4 (4)
C13-N4-C12 / N4-C12-C22	2.4 (6)	4.3 (4)

Selected Dihedral Angles for $Co(C_{22}H_{22}N_4)ICHCl_3$

Atoms defining planes	Angles, deg
C11-C2-N1 / C2-N1-C3	11.5 (5)
C2-N1-C3 / N1-C3-C4	24.8 (6)
C12-C9-N2 / C9-N2-C8	12.7 (6)
C9-N2-C8 / N2-C8-C7	32.2 (6)

Table XIII. Angles between Selected Planes

Defining planes between N1-N2-N3-N4 and	$[Mn(C_{22}H_{22}N_4)\text{-}N(C_2H_5)_3]$	$[Fe(C_{22}H_{22}N_4)Cl]\cdot CH_3CN$
N1-C1-C2-C3-N2	32.77	31.52
N1-C1-C3-N2	33.91	31.70
N3-C10-C11-C12-N4	37.64	34.20
N3-C10-C12-N4	38.89	34.29
N2-C4-C9-N3	11.84	15.87
N1-C18-C13-N4	12.87	16.70
C4-C5-C6-C7-C8-C9	20.62	21.37
C13-C14-C15-C16-C7-C18	20.41	22.22

Angles between Selected Planes for $[Co(C_{22}H_{22}N_4)I]\cdot CHCl_3$

Defining planes between N1-N2-N1(m)-N2(m) and	Angle, deg
N1-C3-C8-N2	16.14
N1-C2-C1-C2(m)-N1(m)	19.76
N2-C9-C10-C9(m)-N2(m)	22.86
C3-C4-C5-C6-C7-C8	21.67

pansion of the Ct-N distance does occur upon coordination of these metals (vide supra). However, the increases are still insufficient to accommodate the larger radii of high-spin Fe(III) and Mn(II), and the difference between the available core size and the real metal-nitrogen distances is accommodated by displacement of the metal from the N_4 plane. The Co(III) atom is 0.234 Å from the N_4 plane, but this displacement is most likely the consequence of the steric interactions and attendant warping of the ligand than to an inability of the Co(III) atom to fit within the N_4 plane. The larger radii associated with Fe(III) and Mn(II) necessitate a greater displacement from the N_4 plane, 0.600 and 0.730 Å, respectively. Without the aforementioned changes in ligand conformation, these displacements would result in a serious mismatch of metal and ligand orbitals.

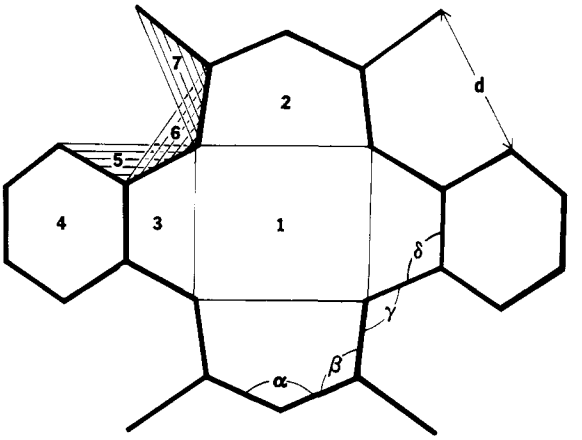

Figure 10. Diagrammatic representation of the $C_{22}H_{22}N_4$ framework with "key" notation to assist the tabulation of the various average parameters listed in Table XIV.

As indicated above, the warping of the macrocyclic ligand parallels the displacement of the M^{n+} from the N_4 donor plane, the N_4 donor pairs remaining nominally pointed toward the metal. The extent of the mismatch can be estimated by considering the average dihedral angle between the planes defined by C-M-C and C-N-C in Figure 11. Assuming sp^2 hybridization of the N atoms and the concomitant ability of the metal orbitals to rehybridize to point at the N atoms, the dihedral angle should be zero for ideal overlap. This is not observed. There is a progression in the size of the dihedral angles between these planes from −1.1° (0° within the experimental measurement) for the Co(III) complex, to 4.70° for the Fe(III) complex, and to a maximum value of 6.6° for the Mn(II) complex, proportional to the metal-N_4 displacement. These trends are consistent with the ease of demetalation of the macrocyclic ligand with anhydrous HCl, in which metal ejection is likely to be associated with increased metal-nitrogen orbital mismatch, thus easing protonation of the ring nitrogens.

Axial Ligation and Comparison with Porphyrin Structures. In all three structures the metal-to-axial ligand bond distances

Table XIV. Summary of Important Parameters for the Three $[M(C_{22}H_{22}N_4)X]$ Structures

	$[Mn(C_{22}H_{22}N_4)N(C_2H_5)_3]$	$[Fe(C_{22}H_{22}N_4)Cl]\cdot CH_3CN$	$[Co(C_{22}H_{22}N_4)I]\cdot CHCl_3$
Av M-N distance, Å[a]	2.118 (2.128)	2.002 (2.05)	1.901 (1.978)
Distance of M from N_4 donor plane, Å[a]	0.730 (0.56)	0.600 (0.38)	0.234 (0.094)
Ct-N distance, Å[a]	1.988 (2.065)	1.910 (2.014)	1.893 (1.976)
M-axial ligand distance	2.253 (3)	2.252 (1)	2.557 (1)
Av C-N distance (six-membered chelate ring)	1.327 (4)	1.331 (3)	1.344 (4)
Av C-C distance (six-membered chelate ring)	1.406 (5)	1.404 (4)	1.382 (4)
Av C-N distance (five-membered chelate ring)	1.403 (4)	1.422 (4)	1.411 (4)
	Average Dihedral Angles, deg[b]		
1-2	35.20	32.86	21.31
1-3	12.36	16.28	16.14
1-4	20.52	21.80	21.67
5-6	51.3	43.5	28.5
6-7	1.6	3.2	12.1
	Average Bond Angle, deg[b]		
α	131.2	129.6	130.2
β	123.1	121.5	121.4
γ	126.3	125.0	123.8
δ	115.6	113.9	113.2
	Average Nonbonded Distance, Å[b]		
d	3.126	3.054	2.949

[a] Numbers in parentheses refer to corresponding distances in [Mn(TPP)(1-MeIM)], $[Fe(TPP)Cl]_2$, and [Co(TPP)(NO)], ref 26, 25, and 27, respectively. [b] See Figure 10 for key.

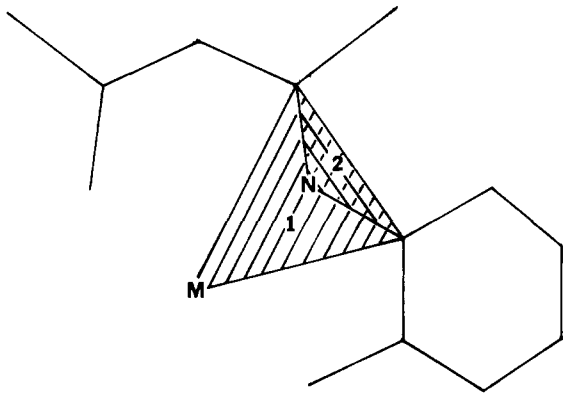

Figure 11. Diagram illustrating the planes used to evaluate the dihedral angles and the extent of the mismatch between the metal and ligand orbitals.

are slightly longer than normal, and longer than for corresponding M–X distances of tetraphenylporphyrin (TPP) complexes. Although no structures containing Co(III)–I bonds have been reported, the intermediate spin configuration vitiates all comparisons with low-spin Co(III) complexes. The occupation of the z^2 orbital leads to a situation somewhat analogous to low-spin cobalt(II) complexes where the occupation of the z^2 orbitals and associated Jahn–Teller effects lead to abnormally long distances to axial ligands. The Fe–Cl distance, 2.252 Å, is 0.06 and 0.03 Å longer than for the corresponding [Fe(TPP)Cl] and α-chlorohemin complexes, respectively;[25] the Mn–N(triethylamine) distance, 2.253 Å, is 0.06 Å longer than the Mn–N(axial) distance in the [Mn(TPP)(1-MeIm)] complex.[26] Since the charge delocalization of the $C_{22}H_{22}N_4^{2-}$ ligand is limited essentially to the six-membered chelate rings and the $M-N_4$ distances are shorter, the charge donation to the metal from the macrocyclic ligand is significantly larger than in the delocalized porphyrin ligands. Thus the electrostatic component to the M–axial ligand bond is expected to be less for the $C_{22}H_{22}N_4^{2-}$ complexes than for porphyrins and lead to longer bond distances.

The general trends of the structural parameters of the inner coordination sphere of these three macrocyclic complexes closely parallel those of related tetraphenylporphyrin complexes. Table XIV lists some of the related parameters from three porphyrin structures, the five-coordinate [Co(III)-TPP(NO)] complex[27] (the only crystal structure of a five-coordinate Co(III) porphyrin), the five-coordinate [Fe(TPP)Cl], and the five-coordinate [Mn(TPP)(1-MeIm)] species. The greatest difference in $M-N_4$ bond length for the two ligand types occurs in the Co(III) complexes, approximately 0.1 Å. This difference results primarily from the much larger N–Ct distance for the porphyrin ligand than for the $C_{22}H_{22}N_4^{2-}$ ligand and the inability of the porphyrin ligand to contract to accommodate the smaller radius of the Co(III). For larger metals such as Fe(III) and Mn(II), the difference between the idealized metal–N distance and the Ct–N distance is accommodated by projecting the metal above the plane and the metal–N distances are much closer in the two ligands, differing by only a few hundreths of an angstrom.

Both ligands have some flexibility with respect to the Ct–N distance. In the Co(III) and the Mn(II) complexes of $C_{22}H_{22}N_4^{2-}$ (and TPP) the Ct–N distances increase from 1.893 (1.976) to 1.988 (2.065) Å, respectively. However, with respect to directional character of the N_4 lone pairs and ligand framework flexibility, the $C_{22}H_{22}N_4^{2-}$ ligand is considerably more flexible for two reasons. First, the various types of angles denoted by α–δ (Figure 10) expand to facilitate a slight radial expansion of the ligand more easily than the porphyrin system. Second, the nominally single C–N bonds of the five-membered rings permit much larger torsional motions than possible in the porphyrin skeleton.

Acknowledgment. This research was supported in part by the National Institutes of Health, Grant No. HL14827. M. C. Weiss is an MSTP trainee supported by U.S. Public Health Service Training Grant No. 5T05 GM 01939 from the NIGMS.

Supplementary Material Available. A listing of hydrogen atom coordinates and the observed and calculated structure factor amplitudes (87 pages). Ordering information is given on any current masthead page.

References and Notes

(1) Address correspondence to this author at the Department of Chemistry, The Florida State University, Talahassee, Fla. 32306.
(2) D. P. Riley, J. A. Stone, and D. H. Busch, *J. Am. Chem. Soc.*, **98**, 1752 (1976); M. C. Weiss and V. L. Goedken, *J. Chem. Soc., Chem. Commun.*, 531 (1976).
(3) L. E. Godycki and R. E. Rundle, *Acta Crystallogr.*, **6**, 487 (1953); G. Basu, G. M. Cook, and R. L. Belford, *Inorg. Chem.*, **3**, 1361 (1964).
(4) E.-G. Jäger, *Z. Chem.*, **4**, 437 (1964).
(5) V. L. Goedken, J. J. Pluth, S.-M. Peng, and B. Bursten, *J. Am. Chem. Soc.*, preceding paper in this issue.
(6) (a) V. L. Goedken and Y. Park, *J. Chem. Soc., Chem. Commun.*, 214 (1975); (b) V. L. Goedken, S.-M. Peng, J. Molin-Norris, an Y. Park, *J. Am. Chem. Soc.*, in press.
(7) D. R. Neves and J. C. Dabrowiak, *Inorg. Chem.*, **15**, 129 (1976).
(8) M. C. Weiss and V. L. Goedken, *J. Am. Chem. Soc.*, **98**, 3389 (1976).
(9) Co(III)–N distances for unsaturated ligands such as dimethyl glyoxime are generally in the range 1.88–1.92 Å: D. Dodd and M. D. Johnson, *Organomet. Chem. Res.*, **52**, 34 (1973); S. Bruckner and L. Randaccio, *J. Chem. Soc., Dalton Trans.*, 1017 (1974); R. K. Murmann and E. O. Schlemper, *Inorg. Chem.*, **12**, 2625 (1973); L. P. Battaglia, A. B. Corradi, C. G. Palmieri, M. Mardelli, and M. E. V. Tani, *Acta Crystallogr.*, **30**, 1114 (1974). Co(III)–N distances for saturated ligands are normally in the range of 1.95–2.00 Å: D. A. Snyder and D. L. Weaver, *Inorg. Chem.*, **9**, 2760 (1970); R. Stomberg and I. Larking, *Acta Chem. Scand.*, **23**, 343 (1969); O. Bortin, *Acta Chem. Scand.*, **23**, 3273 (1969); A. Muto, F. Marumo, and Y. Saito, *Acta Crystallogr., Sect. B*, **26**, 226 (1970).
(10) M. Di Vaira and P. L. Orioli, *Acta Crystallogr., Sect. B*, **24**, 1269 (1968); S. J. Rettig and J. Trotter, *Can. J. Chem.*, **51**, 1303 (1973); S. Richards, B. Pederson, J. V. Silverton, and J. L. Hoard, *Inorg. Chem.*, **3**, 27 (1964).
(11) J. L. Hoard, *Science*, **174**, 1295 (1971).
(12) The possibility of the CH_3CN interacting with the metal complex was prompted by our observation that some six-coordinate cobalt(III) complexes derived from this ligand crystallize with CH_3CN in the lattice. The NMR spectra of these compounds exhibit a broad CH_3CN ^1H NMR resonance at 1.50 ppm, strongly suggesting an interaction with the complexes in solution (see ref 8).
(13) V. L. Goedken and J. Molin-Case, *J. Chem. Soc., Chem. Commun.*, 337 (1973).
(14) (a) "International Tables for X-Ray Crystallography", 2d ed, Vol. I, Kynoch Press, Birmingham, England, 1965, p 99; (b) *ibid.*, p 141.
(15) The obtainment of the refined lattice constants and the data collection was facilitated with the automatic diffractometer control programs of Lenhert. P. G. Lenhert, *J. Appl. Crystallogr.*, **8**, 568 (1975).
(16) L. V. Azaroff, *Acta Crystallogr.*, **8**, 701 (1955).
(17) W. Busing and H. A. Levy, *J. Chem. Phys.*, **26**, 563 (1957); P. W. R. Corfield, R. Doedens, and J. A. Ibers, *Inorg. Chem.*, **6**, 197 (1967).
(18) Computations were performed by IBM 370 computer with the aid of the following programs: Zalkin's FORDAP Fourier program, Busing and Levy's ORFFE function and error program, and Ibers NUCLS least-squares program. Plots of the structures were drawn with the aid of C. K. Johnson's ORTEP.
(19) Neutral atom scattering factors were taken from D. T. Cromer and J. B. Mann, *Acta Crystallogr., Sect. A*, **24**, 321 (1968). Hydrogen atom scattering factors were taken from "International Tables for X-Ray Crystallography", Vol. III, Kynoch Press, Birmingham, England, 1962. Anomalous scattering corrections were applied to heavy atoms and were taken from D. T. Cromer, *Acta Crystallogr.*, **18**, 17 (1965).
(20) M. R. Churchill, *Inorg. Chem.*, **12**, 1213 (1973).
(21) See paragraph at the end of this paper regarding supplementary material.
(22) The average C–N bond length of the five-membered chelate ring of $[Ni(C_{18}H_{14}N_4)]$, an analogous dibenzo[14]annulene complex devoid of methyl groups with a planar structure, is 1.418 Å: M. C. Weiss, G. Gordon, and V. L. Goedken, submitted for publication.
(23) D. Lloyd and D. R. Marshall, *Jerusalem Symp. Quantum Chem. Biochem.*, **4**, 85 (1971).
(24) A single axial ligand or a ligand with strong π-acceptor properties will tend to pull the metal atom out of the N_4 donor plane by a few tenths of angstrom.
(25) J. L. Hoard, G. H. Cohen, and M. D. Glick, *J. Am. Chem. Soc.*, **89**, 1922 (1967); D. F. Koenig, *Acta Crystallogr.* **18**, 663 (1965).
(26) B. Gonzalez, J. K. S. Yee, C. Reed, J. F. Kirner, and W. R. Scheidt, *J. Am. Chem. Soc.*, **97**, 3247 (1975).
(27) W. R. Scheidt and J. L. Hoard, *J. Am. Chem. Soc.*, **95**, 8281 (1973).